Electronic Supplementary Material (ESI) for Journal of Materials Chemistry A.

Supporting Information

High-Performance Carbon Nanotube-Cellulose Nanofiber Bulk Materials with Thermal Management and Electromagnetic Interference Shielding Multifunctional Applications

Xiao Feng[a], Xijun Wang[a], Ming Wang[a], Shenming Tao[a], Yian Chen[a], Haisong Qi[a,*]

[a] *State Key Laboratory of Pulp and Paper Engineering, South China University of Technology, Guangzhou 510640, China.*

* *Corresponding Author*

E-mail: qihs@scut.edu.cn

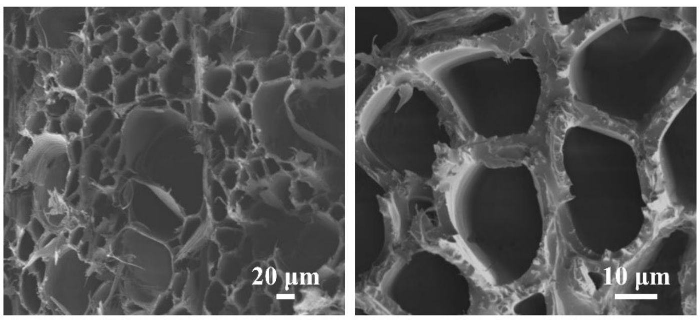

Fig. S1 SEM images of lumina of basswood in the transverse section.

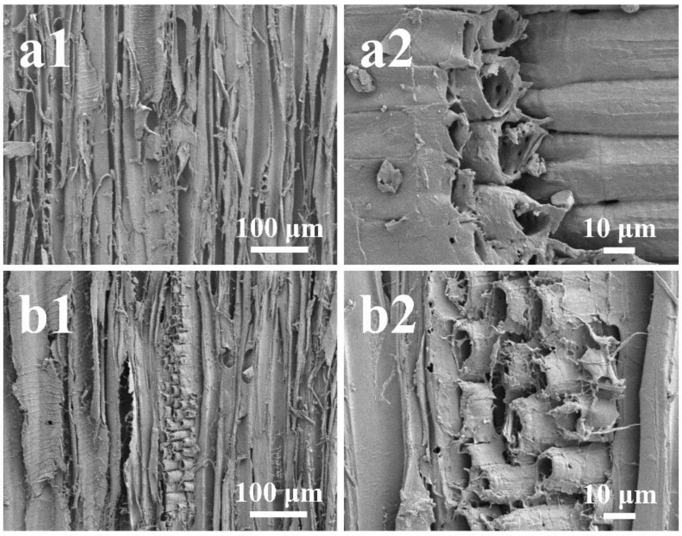

Fig. S2 SEM images of basswood veneers (a) before and (b) after chemical pretreatment.

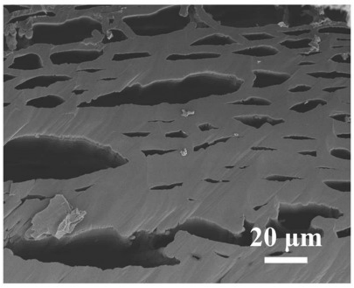

Fig. S3 SEM image of a cross-section of purely mechanically pressed basswood without chemical pretreatment.

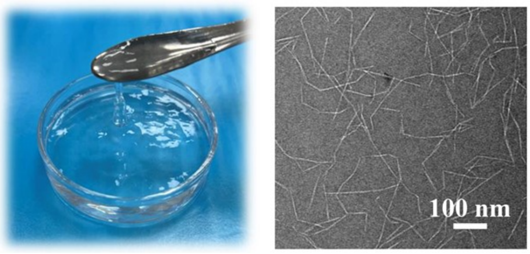

Fig. S4 Digital and TEM images of CNF dispersion.

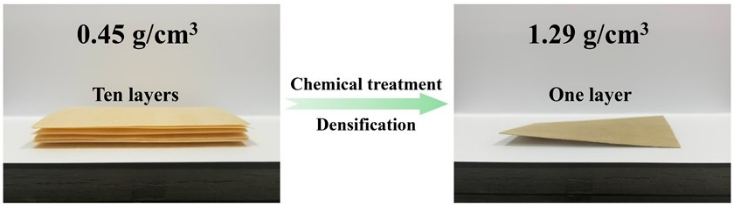

Fig. S5 Digital photos of $CCNB_0$ made from ten layers of basswood veneers.

Table S1 Degree of substitution (*DS*) and surface charge density of CNFs.

Sample	Sulfur content (%)	Surface charge density ($-SO_4^-$)	*DS*	Dispersion limit (CNT:CNF)
CNFs	7.574	2362 μmol/g	0.497	4:1 (80 wt% CNTs)

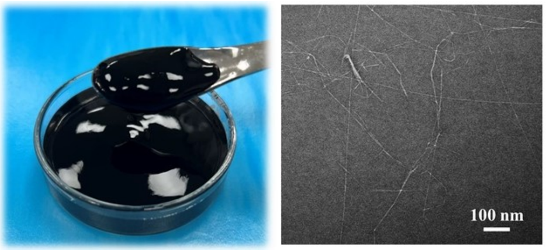

Fig. S6 Digital and TEM images of CNT-CNF dispersion.

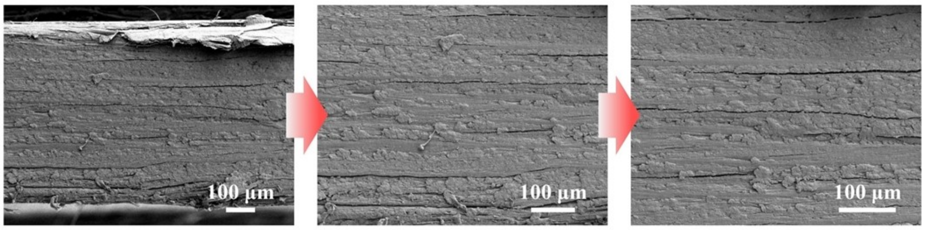

Fig. S7 SEM images of the conductive multilayer structure of CCNBs.

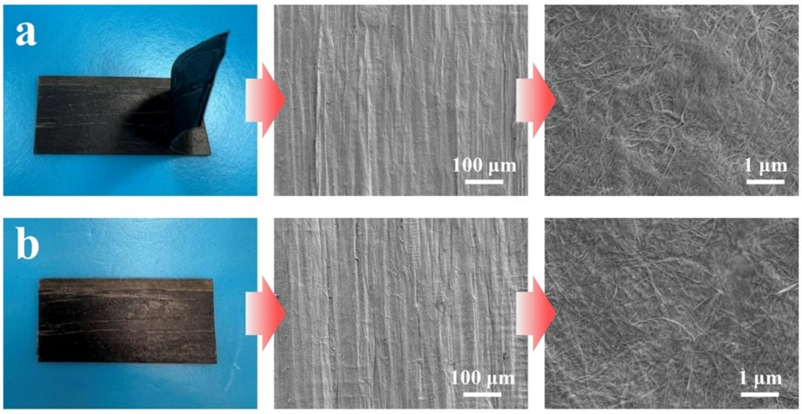

Fig. S8 Digital photo and SEM images of the exposed CNT-CNF conductive layer inside CCNBs (a) before and (b) after adhesive tape peeling.

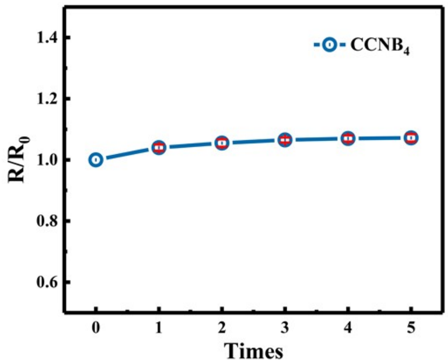

Fig. S9 Changes in relative resistance of CNT-CNF conductive layers after 5 peel tests.

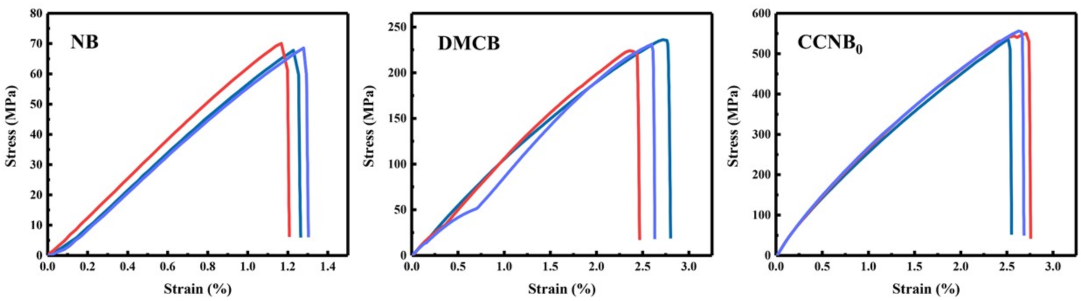

Fig. S10 Tensile stress-strain curves of NB, DMCB and $CCNB_0$.

Table S2 Tensile strength and Young's modulus of $CCNB_0$ compared with other nanocellulose materials.

Materials	Tensile strength	Young's modulus
All-cellulose composite [1]	480	20
Cellulose nanopaper [2]	214	13.2
TEMPO-NFC nanopaper [3]	430	33
Wood cellulose biocomposites [4]	256	13.8
CNF-g-PEG [5]	487	22.1
Self-reinforced cellulose films [6]	430	33
Aligned BC arrays [7]	285	18.4
TEMPO-Oxidized CNF films [8]	277	8.3
Transparent cellulose films [9]	150	6
Nanofibrillated cellulose films [10]	474	46
$CCNB_0$	**502**	**31.8**

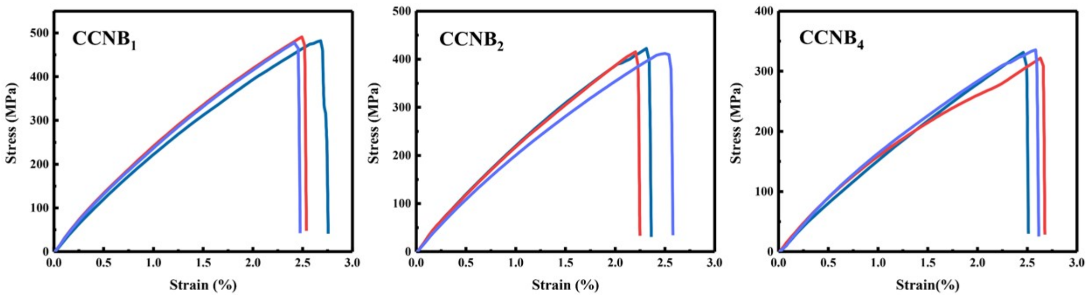

Fig. S11 Tensile stress-strain curves of $CCNB_1$, $CCNB_2$ and $CCNB_4$.

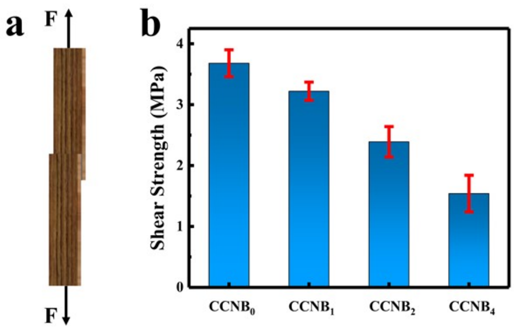

Fig. S12 (a) Schematic illustration of the shear strength test of CCNBs. (b) Shear strength of

CCNBs.

Table S3 The addition amount of CNFs and CNTs in CCNBs.

Materials	CNTs		CNFs	
	g/m²	**wt%**	**g/m²**	**wt%**
$CCNB_0$-5	0	0	2.34	0.75
$CCNB_0$-10	0	0	4.68	0.825
$CCNB_1$-5	2.34	0.75	2.34	0.75
$CCNB_1$-10	4.68	0.825	4.68	0.825
$CCNB_2$-5	4.68	0.825	2.34	0.75
$CCNB_2$-10	9.375	1.65	4.68	0.825
$CCNB_4$-5	9.375	1.65	2.34	0.75
$CCNB_4$-10	18.75	3.3	4.68	0.825

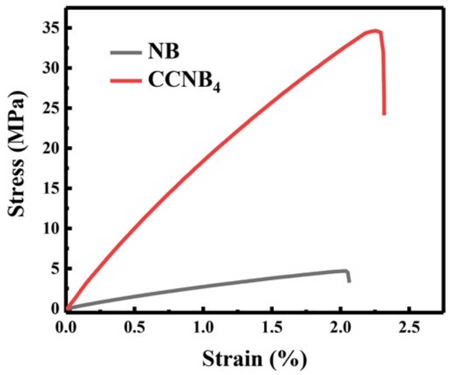

Fig. S13 Tensile strength curves of NB and $CCNB_4$ perpendicular to the growth direction.

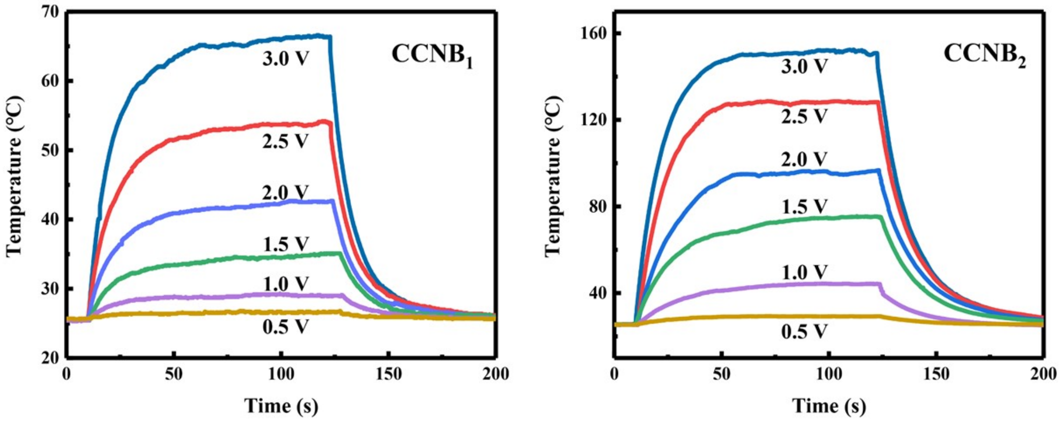

Fig. S14 The temperature curves of $CCNB_1$ and $CCNB_2$ at different working voltages.

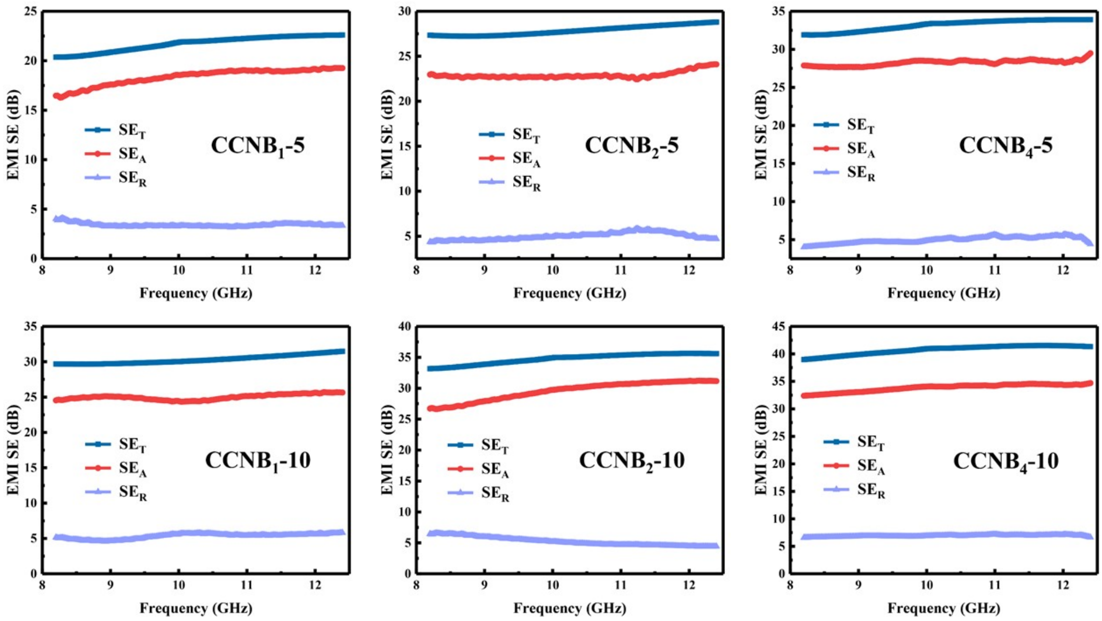

Fig. S15 SE_T, SE_A, and SE_R of CCNBs.

Table S4 Summary of EMI shielding performance of cellulose-based composites.

Materials	EMI SE (dB)	Thickness (mm)	Density (g cm^{-3})	SSE/t (dB cm^2 g^{-1})	σ (S/cm)	Strength (MPa)	Conductive fillers loading
CNTs/RGI-wood[11]	90	2	1.35	333	~ 10	170	18.5 vol%
AgNWs/GNSs/cellulose[12]	53.3	0.17	-	-	26.87	35.27	3.98 wt%
CNTs/MXene/CNFs[13]	38.4	0.038	1.26	8020	25.07	97.9	~ 80.5 wt%
CNF/rGO aerogels[14]	32	3.023	0.0035	30000	0.55	< 0.01	50 wt%

BC-buckypaper[15]	24.01	0.036	0.735	9074	16.67	55.78	50 wt%
	29.12	0.044	0.687	9624	27.78	< 20	80 wt%
CNFs/CNT/$Ti_3C_2T_x$[16]	20.5	0.012	1.83	9316.4	3650	~ 50	80 wt%
PLA/CNC/CNT[17]	41.8	1.5	-	-	1	45.52	4.3 wt%
NFC/CNT foams[18]	70	8	0.018	6111	5.2	< 0.015	67 wt%
CNTs/cellulose films[19]	35	0.15	1.7	1372.4	20	26.9	40 wt%
SWCNT/cellulose film[20]	35	0.031	1.48	7678	5	~ 90	10 wt%
NFC/Fe_3O_4/CNT/PEO[21]	50	30.3	-	-	39	36.03	~ 50 wt%
CNT/Cellulose composite[22]	40	2.5	0.077	2078	0.39	0.58	0.51 vol%
$CCNB_1$-10	30.3	0.44	1.29	534	4.6	483	~ 0.825 wt%
$CCNB_2$-10	34.8	0.44	1.29	613	17.2	416	~ 1.65 wt%
$CCNB_4$-10	40.7	0.44	1.29	717	54.2	330	~ 3.3 wt%

Experimental section

The electrical conductivity of CCNBs was calculated according to the formula:

$$\sigma = \frac{L}{R \times S}$$

where σ was the electrical conductivity, R was the resistance of the sample, S was the cross-sectional area of the sample, and L was the length of the test sample.

During the mechanical properties test of basswood veneers and CCNBs, the stretching rate is 5 mm·min^{-1} in a standard environment (T = 23°C, relative humidity = 50%). The length and width of CCNBs were 100 mm and 5 mm, respectively.

For the lap shear tests, CNT-CNF dispersions were applied on a veneer (8 cm × 2 cm × 0.02 cm). The other veneer with the same dimensions was left to rest on the dispersion and maintained homogeneous, planar, level contact between the adhering surfaces. The overlap area was typically 1 cm × 1.5 cm. A hot-pressing step with a pressure of 1 MPa was applied at 100°C until the samples were dried. The gauge length was 70 mm and the strain rate was 5 mm/min.

The diameter of CCNBs used for the EMI shielding performance test was about 10 mm. The total EMI SE (SE_T) values were the sum of the multiple internal reflections of microwaves (SE_M), the absorption of electromagnetic energy (SE_A), and the reflection (SE_R). Reflectivity (R), absorptivity (A), and transmissivity (T) were determined based on the measured S parameters (S_{11} and S_{12}): $R = S_{11}^2$, $T = S_{12}^2$, and $A = 1 - R - T$. SE_T, SE_A, and SE_R were calculated according to the followed calculations:

$$SE_T = -10 \log T$$

$$SE_R = -10 \log (1 - R)$$

$$SE_A = SE_T - SE_R - SE_M$$

When $SE_T \geq 15$ dB, SE_M could be ignored.[23]

The EMI shielding efficiency was calculated by the following equation:[24]

$$Shielding\ efficiency\ (\%) = 100 - \left(\frac{1}{10^{SE/10}}\right) \times 100$$

In order to comprehensively compare the effectiveness of shielding materials, density and thickness of the materials were also considered.[13] The related equations were described as:

$$SSE = \frac{EMI\ SE}{Density}$$

$$SSE/t = \frac{SSE}{Thickness}$$

References

[1] T. Nishino, I. Matsuda and K. Hirao, *Macromolecules*, 2004, **37**, 7683-7687.

[2] M. Henriksson, L. A. Berglund, P. Isaksson, T. Lindström and T. Nishino, *Biomacromolecules*, 2008, **9**, 1579-1585.

[3] H. Sehaqui, N. Ezekiel Mushi, S. Morimune, M. Salajkova, T. Nishino and L. A. Berglund, *ACS Appl. Mater. Interfaces*, 2012, **4**, 1043-1049.

[4] H. Sehaqui, M. Allais, Q. Zhou and L. A. Berglund, *Compos. Sci. Technol.*, 2011, **71**, 382-387.

[5] H. Tang, N. Butchosa and Q. Zhou, *Adv. Mater.*, 2015, **27**, 2070-2076.

[6] W. Gindl and J. Keckes, *J. Appl. Polym. Sci.*, 2007, **103**, 2703-2708.

[7] M. M. Rahman and A. N. Netravali, *ACS Macro Lett.*, 2016, **5**, 1070-1074.

[8] H. Fukuzumi, T. Saito, T. Iwata, Y. Kumamoto and A. Isogai, *Biomacromolecules*, 2009, **10**, 162-165.

[9] Q. Yang, H. Fukuzumi, T. Saito, A. Isogai and L. Zhang, *Biomacromolecules*, 2011, **12**, 2766-2771.

[10] C. Baez, J. Considine and R. Rowlands, *Cellulose*, 2014, **21**, 347-356.

[11] Q. Guan, Z. Han, H. Yang, Z. Ling and S. Yu, *Natl. Sci. Rev.*, 2021, **8**, nwaa230.

[12] F. Zhang, P. Ren, H. Guo, Z. Zhang, Z. Guo, Z. Dai, Z. Lu, Y. Jin and F. Ren, *Adv. Electron. Mater.*, 2021, **7**, 2100496.

[13] W. Cao, C. Ma, S. Tan, M. Ma, P. Wan and F. Chen, *Nano-Micro Lett.*, 2019, **11**, 72.

[14] M. Li, M. Zhang, Y. Zhao, S. Jiang, Q. Xu, F. Han, J. Zhu, L. Liu and A. Ge, *Carbohyd. Polym.*, 2022, **286**, 119306.

[15] M. Fan, X. Xia, S. Li, R. Zhang, L. Wu, M. Qu, P. Tang and Y. Bin, *Chem. Eng. J.*, 2022, **441**, 136103.

[16] L. Zhang, S. Yang, L. Li, B. Yang, H. Huang, D. Yan, G. Zhong, L. Xu and Z. Li, *ACS Appl. Mater. Interfaces*, 2018, **10**, 40156-40167.

[17] B. Yu, Z. Zhao, S. Fu, L. Meng, Y. Liu, F. Chen, K. Wang and Q. Fu, *Compos. Part A Appl. Sci. Manuf.*, 2019, **125**, 105558.

[18] Z. Zeng, C. Wang, T. Wu, D. Han, M. Lukovi, F. Pan, G. Siqueira and G. Nyström, *J. Mater. Chem. A*, 2020, **8**, 17969-17979.

[19] L. Zhang, B. Yang, J. Teng, J. Lei, D. Yan, G. Zhong and Z. Li, *J. Mater. Chem. C*, 2017, **5**, 3130-3138.

[20] X. Feng, X. Qin, D. Liu, Z. Huang, Y. Zhou, W. Lan, F. Lu and H. Qi, *Macromol. Mater. Eng.*, 2018, **303**, 1800377.

[21] Y. Li, B. Xue, S. Yang, Z. Cheng, L. Xie and Q. Zheng, *Chem. Eng. J.*, 2021, **410**, 128356.

[22] L. Zhang, S. Yang, L. Li, B. Yang, H. Huang, D. Yan, G. Zhong, L. Xu and Z. Li, *ACS Appl. Mater. Interfaces*, 2018, **10**, 40156-40167.

[23] Y. Chen, Y. Li, Y. Liu, P. Chen, C. Zhang and H. Qi, *ACS Appl. Mater. Interfaces*, 2021, **13**, 36221-36231.

[24] Y. Li, Y. Chen, X. He, Z. Xiang, T. Heinze and H. Qi, *Chem. Eng. J.*, 2022, **431**, 133907.